7.5 WIND SHELTERING OF SMALL LAKES BY COMPLEX TERRAIN

Corey D. Markfort[a]*, E. L. Resseger[a], W. Zhang[a], F. Porté-Agel[b] and H. G. Stefan[a]
[a]University of Minnesota, Minneapolis, Minnesota
[b]EPFL, Lausanne, Switzerland

1. Introduction

1.1 *Lake-Atmosphere Interaction*

Land-atmosphere interactions are characterized by the fluxes of momentum, sensible heat, water vapor, and trace gases between the Earth's surface and the atmosphere. Lakes are an important "land" surface type. There are approximately 304 million lakes in the world, covering about 3% of the Earth's terrestrial surface (Downing et al., 2006). Most lakes have a surface water area less than 10 km^2. Having a lower albedo and larger heat capacity than land, lakes absorb more solar radiation and store more heat, and often have a surface temperature different from the surrounding landscape. Lakes may be a source or sink of sensible heat and often are a source of moisture to the atmosphere. Lake surfaces are aerodynamically much smoother than vegetated land surfaces, which contributes to large variations of fluxes of momentum, heat, moisture and gases between the landscape and the atmospheric.

Not only physical processes, but also biological and chemical processes in lakes are strongly influenced by atmospheric forcing including energy exchange, and many processes are mediated by turbulence, either in the air or in the water. Components of the energy budget, which are strongly affected by airside boundary layer turbulence include the sensible and latent heat fluxes. Trace gas transfer (e.g. O_2, CO_2 and CH_4, compounds important to biological processes in the lake as well as climate processes) at the water surface is strongly influenced by waterside turbulence near the surface. Lake processes that are particularly affected by turbulence are the momentum and heat fluxes. The one-dimensional (1-D) momentum, moisture and sensible heat fluxes can be formulated in terms of turbulent fluxes or modeled in terms of mean components as

$$\tau = \rho_a \overline{u'w'} = \rho_a C_D \bar{u}^2, \quad (1)$$

$$LE = \rho_a L_v \overline{w'q'} = \rho_a L_v C_E \bar{u}(q_s - q_a), \quad (2)$$

$$H = \rho_a c_p \overline{w'\theta'} = \rho_a c_p C_H \bar{u}(\theta_s - \theta_a), \quad (3)$$

respectively. The coefficients C_D, C_E and C_H are the drag, moisture transfer and sensible heat transfer coefficients for τ, LE and H, respectively; ρ_a is the density of air, u and w are the streamwise (horizontal) and vertical instantaneous velocities, q is the specific humidity, θ is the temperature, L_v is the latent heat of vaporization, and c_p is the specific heat at a constant pressure. The subscripts s and a signify whether the quantity is in the air or in the water, and an overbar, e.g. $\overline{u}$ means temporal averaging while primes indicate fluctuating quantities.

* *Corresponding author address:* C.D. Markfort, Saint Anthony Falls, 2 3rd Avenue SE, Minneapolis, MN 55414, e-mail: mark0340@umn.edu, Web: http://umn.edu/∼mark0340

The inclusion of lakes in weather and climate models will most likely improve the accuracy of simulated land-atmosphere interactions. Formulations of estimates of lake-atmosphere fluxes are often taken from experimental studies conducted on oceans or on lakes where the wind sheltering effects are not significant. The same coefficients values are most likely not applicable to all lake environments, especially over the many small lakes with different sheltering characteristics. The accuracy and variability of transfer coefficients for air-water momentum, heat, moisture and trace gases is currently difficult to determine and any bias in them will propagate directly to the flux estimates.

Wind shear stress on the water surface drives turbulent kinetic energy into the surface layer of a lake and leads to mixing of thermally stratified water (Stefan and Ford, 1975). Several examples of the mixing of warm surface water with cooler water below are shown in the lake temperature record in Figure 1 for Trout Lake, Minnesota. Wind events with elevated u_*-values can be seen to coincide with destratification and deepening of the thermocline from less than 5 m in early July to about 7 m depth in September.

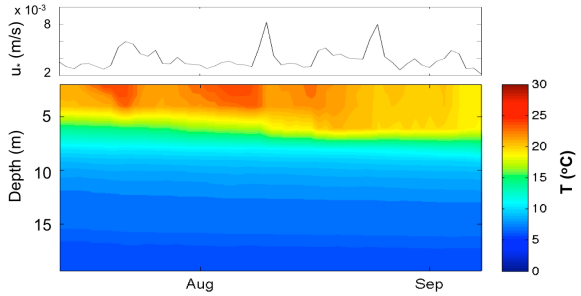

FIG. 1: Plot of wind friction velocity record (top) and countours of temperature (isotherms) versus depth (bottom) for Trout Lake, Minnesota, (from a Field Study in 2011)

The TKE input through the surface of a lake can be modeled as

$$TKE = W_{str} \int_{A_{lake}} u_* \tau dA \approx W_{str} A_{lake} \rho_a u_*^3 \quad (4)$$

where $u_* = \sqrt{\tau/\rho}$, is the friction velocity, A_{lake} is the lake water surface area and W_{str} is a reduction coefficient that accounts for wind sheltering.

Often the value of this wind sheltering coefficient for a specific lake must be determined by calibration of simulated lake temperature profiles against measured ones. There is currently no process based model for the prediction of wind sheltering coefficients, i.e. how wind velocities over a lake may differ from wind measured at a

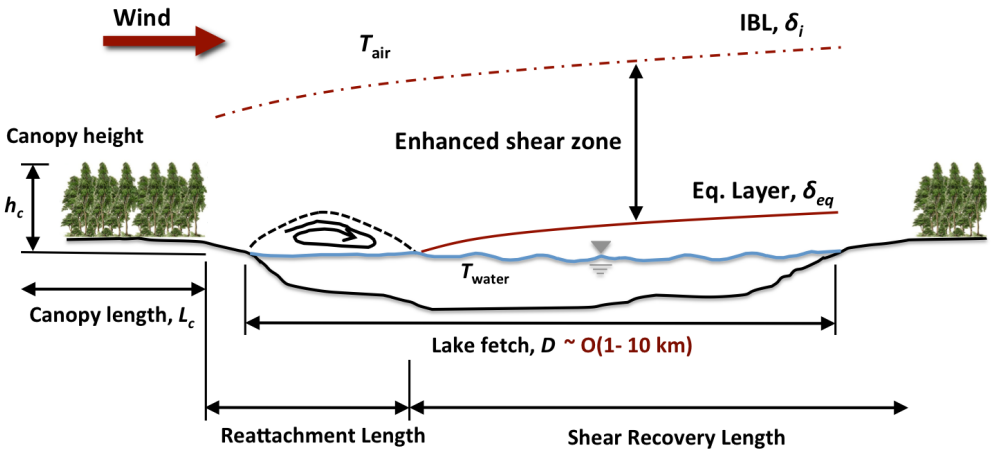

FIG. 2: Schematic of flow transition from a tall canopy to a small lake

nearby weather station or even at some position on the lake itself. The overall objective of this research is to develop a better understanding of the wind sheltering of small lake surfaces by trees (canopies) on the surrounding land.

1.2 *Land-Atmosphere-Lake Interaction*

Lakes are affected by the landscape that surrounds them in many ways. In flat terrain the and for a relatively large lake, the transition between land and lake may be characterized in its simplest form as a rough to smooth transition (Garratt, 1994). Forest canopies surrounding a small lake in flat terrain may affect the wind field over the lake more strongly than a roughness transition due to the wake formed downwind of the canopy. The flow behind a tree canopy may be more similar to the flow behind a backward-facing step (BFS) (Detto et al., 2008), and the flow may separate forming a recirculation zone (see Figure 2). However, the density, height and length of the canopy, may all significantly alter the flow separation and reattachment.

At the point where the air flow reattaches to the water surface, the surface shear stress is, by definition, zero. Downwind of the reattachment, the shear stress increases towards an equilibrium value and a new equilibrium layer forms. Above this equilibrium layer is a wake region of low velocity and high turbulence generated by the shear layer between the wake region and the high-speed flow above. The wake zone behind the canopy strongly effects the flow over the lake surface and the distance required for the boundary layer to adjust. Because the roughness of the lake is significantly less than the roughness of the canopy, and because of the separation of the flow downstream from the canopy, a variety of initial conditions for the development of the equilibrium layer and surface shear stress may exist. This may lead to a long adjustment length, and for lakes with less than $\approx$ 1 km fetch, there may not be a point on the lake where an adjusted wind can be measured. How and where the wind speed and shear stress on a lake surface are determined is an important and difficult consideration due to the effects of flow separation and the developing boundary layer. It may be possible to model the developing boundary layer using classical theories. However, first we must determine the reattachment location and the variables which control it.

Wind speed records to determine the wind stress over a lake are commonly obtained from the nearest meteorological station, either mounted on the lake or often at an airport. The difficult question is how to adjust the recorded wind to the conditions expected over the entire lake surface. A first simplified approach is to apply a linear factor to the measured wind. However, it is not clear what the factor should be, taking into account the size and shape of a lake as well as the land cover and topography surrounding the lake. To investigate the effect of wakes on lakes with limited fetch, experiments were performed on an ice-covered lake in central Minnesota to measure the wind field and surface shear stress downwind of a canopy (Markfort et al., 2010). Experiments were also performed in the St. Anthony Fall Laboratory boundary layer wind tunnel to measure how canopy length and density effects the shear stress development downwind of a canopy or bluff topography at the shoreline. It was found, based on the field and wind tunnel experimental data, that shear stress recovers after 40 to 60h_c or a nominal distance of 50h_c from the shoreline, where h_c is the height of the canopy and topography above the water surface.

Figure 3 shows a schematic plot of the shear stress recovery at the water surface of a sheltered lake, where the shear stress grows from zero at some reattachment distance from shore to an equilibrium value downwind at approximately $x_\tau \approx 50h_c$. Also show is an model for the total kinetic energy (TKE) delivered to the water surface layer by the wind shear. A simple step function is adopted, which assumes TKE is zero upwind of x_τ and is at an equilibrium value downwind. Assuming an idealized circular lake, with diameter D, based on the actual lake surface area, and by offsetting the circle by x_τ, the overlapping area is considered the area of wind access,

$$A_{\text{windaccess}} = \frac{1}{2}D^2 \cos^{-1}\left(\frac{x_\tau}{D}\right)\sqrt{D^2 - x_\tau^2}. \qquad (5)$$

The ratio of this area to the total lake surface area is taken as the wind sheltering coefficient,

$$W_{str} = \frac{A_{\text{windaccess}}}{A_{\text{lake}}} = \frac{2}{\pi}\cos^{-1}\left(\frac{x_\tau}{D}\right) - \left(\frac{2x_\tau}{\pi D^2}\right)\sqrt{D^2 - x_\tau^2}. \quad (6)$$

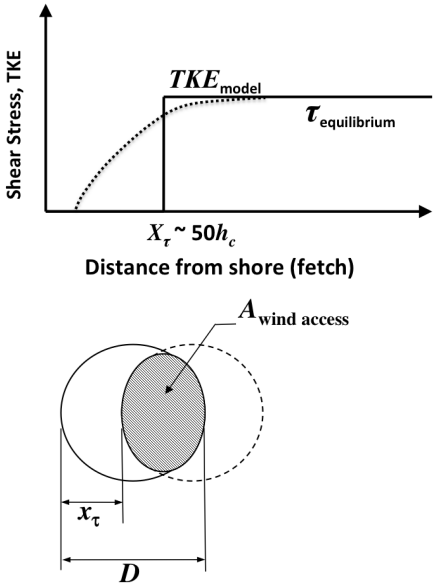

FIG. 3: Schematic of model for total kinetic energy (TKE) input and shear stress downwind of a canopy

A number of lakes have been modeled recently with the 1-D hydrothermal model, MINLAKE2010, to assess the effects of potential climate warming on lake fish habitat (Jiang et al., 2012). Figure 4 shows a comparison between Eqn. 6 and field-calibrated W_{str} values based on numerous temperature profiles measured in each lake and simulated using MINLAKE2010. The wind velocities used for each lake were measured at a nearby airport, and the model was run at a time-step of 24 hrs (Fang et al., 2010). It can be seen that the model does reasonably well for predicting W_{str} for 1-D applications. Equation 6 provides a good survey level approach for the modeling of lake when calibration data are not available. For lakes of a mean diameter that is within approximately 100 times the canopy height, the accuracy of the model (Eqn. 6) is reduced because the specific structure of the sheltering elements becomes increasingly important. The current form of the model is not useful for lakes with highly irregular or oblong shapes, where wind sheltering may depend strongly on wind direction. Islands also have a large effect on sheltering. For 3-D lake models, a complete spatial-temporal characterization of the wind shear is required.

For small lakes, the specific structure of the canopy, including its density, length and height must be considered because the wake structure depends strongly on these characteristics, particularly in the near-wake region. Wind measurements made on a small lake show that the wind-field may be significantly different from the spatially averaged wind over the lake. Interpretation of wind measurements and adjustments for wind sheltering

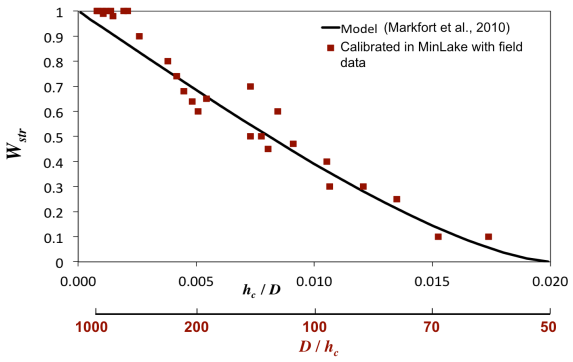

FIG. 4: Plot of wind sheltering coefficient W_{str} based on Eqn. 6 and data from MINLAKE2010 lake temperature model calibrations for individual lakes. Wind sheltering coefficients are plotted vs. the ratio of canopy height h_c to lake diameter D

effects require further detailed investigation. The next step is to characterize how different canopies affect the ABL transition from land to lakes, to improve parameterizations for 1-D lake-atmosphere flux models and to provide guidance for wind measurements on lakes.

2. Wind Tunnel Experiments

To investigate the range of separation scales forming behind canopies, we conducted additional wind tunnel experiments with a number of different model canopies in the St. Anthony Falls Laboratory thermally controlled boundary layer wind tunnel at the University of Minnesota. The wind tunnel was operated in closed-return mode, has a test section length of 16 m and cross section of 1.7 x 1.7 m^2. The experiments presented here involve the flow over and downwind of a long canopy where the flow has fully adjusted, and the flow over a canopy patch with a length to height ratio of 2:1. Results were compared to the flow downwind of a solid backward-facing step (BFS) and over a solid block. The BFS data were taken from Driver and Seegmiller (1985). Their experiments were performed in a wind tunnel at NASA Ames using the LDV method to measure the flow. Oil film interferometry and Preston tube were used to measure surface shear stress.

Our measurements for the canopy-type BFS (Canopy-BFS) were made using primarily two methods. In the near-wake, where separation may occur, the flow was measured using 2-D PIV. In the far-wake region, downwind of reattachment, the flow was measured using high-speed hotwire anemometry. Additionally, measurements were made with a Pitot-static tube of the mean flow and calibration of the x-wire. A Preston tube was used to directly measure the surface shear stress. Here we present results for the near-wake to characterize the flow structure, including where separation occurs and the location of reattachment for the BFS and Canopy-BFS. We also present surface shear stress measurements downwind of reattachment to characterize the recovery of surface shear stress in the newly adjusting boundary layer. A schematic is presented in Figure 5 showing the configuration of the setup in the test section of the wind tunnel.

The flow was tripped allowing a thick boundary layer to developed to approximately $\delta = 60$ cm high over the

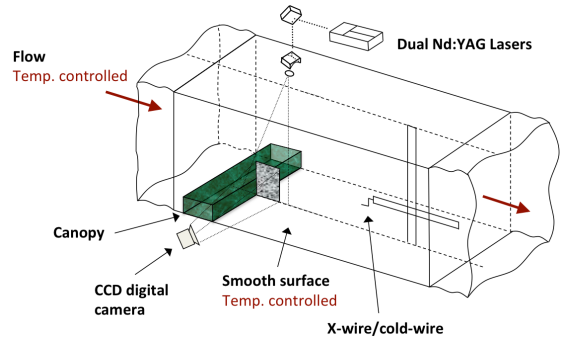

FIG. 5: Schematic of the wind tunnel test section experimental apparatus and instrumentation

canopy. The mean free-stream velocity was controlled at 2 m/s. The canopy model consisted of an array of 10 cm long wooden cylinders with diameter $d = 0.63$ cm. They were mounted in a staggered arrangement on a baseboard 0.7 cm thick. The model extended the full width across the wind tunnel test section and had a total length of 2.5 m. Therefore the length of the canopy, $L = 25h_c$, the density $a = 10$ m^{-1} and a drag development length scale $L_c/L = 0.08$. The drag length scale L_c is defined as $C_D a$. This provided a long enough distance for the flow within the canopy to become fully developed (Belcher et al., 2012). The shear penetration scale into the canopy was approximately $L_s/h_c = 0.5$ (Ghisalberti, 2009). The flow through and over the canopy generally followed the classic structure as presented by Finnigan (2000) and Dupont and Brunet (2009). Details for other experiments, which are compared in this study can be found in Table 1. The leaf area index is characterized as LAI $= ah_c$.

3. Results

3.1 *Flow Separation and Near-Wake Turbulence Fields*

Figure 6 shows the mean streamwise velocities (normalized by the mean freestream velocity) and streamlines for the flow over the BFS and the Canopy-BFS. Two key features are apparent. The separation of the BFS occurs immediately at the edge of the step, while the separation is delayed $\approx 0.5h_c$ for the Canopy-BFS, primarily due to leakage flow through the canopy. The flow reattachment scales are also quite different, with the reattachment occurring at $x_r/h = 6.2$ for the BFS case and at $x_r/h_c = 2.6$ downwind of the Canopy-BFS. The flow in the near-wake for both cases has a significant momentum deficit, the recovery of which is aided by high shear in the flow over the Canopy-BFS compared to the BFS case (Figure 7).

Table 1: Comparison of model characteristics

	L/h_c	LAI	L/L_c	L_s/h_c
BFS	80	—	—	0
Canopy-BFS	25	1.0	12.5	0.5
Canopy-Patch	2	1.8	2	0.34
Solid Block	2	—	—	—

The higher shear over the canopy is due to the porosity of the canopy allowing some flow to go through. The momentum flux leading to flow reattachment can be scaled as $h_c U_h/u_*$ (Belcher et al., 2003). The scales of separation and reattachment for these and for flows over a limited patch of canopy (Canopy-Patch) and solid block, of similar dimensions to the model presented here, are summarized in Table 2.

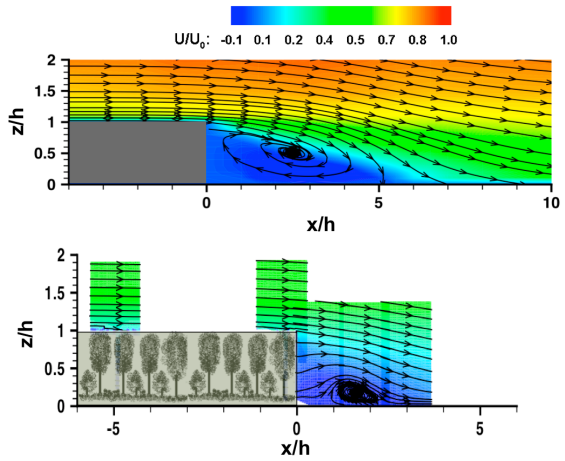

FIG. 6: Normalized mean velocity and streamlines for the flow over the solid BFS (top) and the Canopy-BFS (bottom)

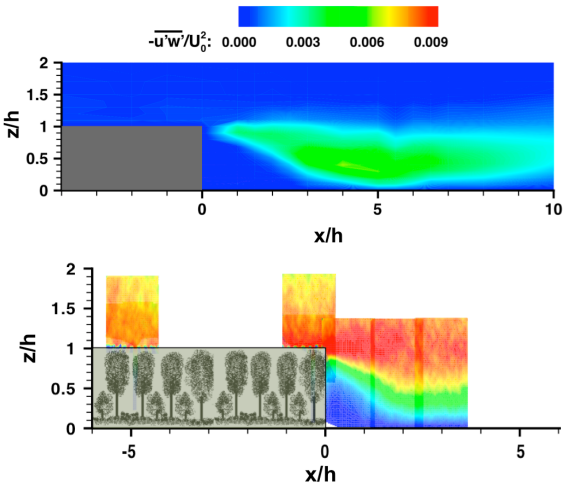

FIG. 7: Normalized shear stress in the flow over the solid BFS (top) and the Canopy-BFS (bottom)

Figure 8 shows a true-color aerial photograph of a small lake surrounded by a forest canopy. Surface wind shear is made visible by the development of a wave field that is reflecting light from the sun. In the nearshore region on the windward side of the lake, the water is flat (no waves) due to a lack of wind shear for a distance of approximately $3h_c$, which is similar to the reattachment length measured for the flow behind the Canopy-BFS. The sun light reflecting off waves makes apparent where shear stress is applied at the water surface of this small lake.

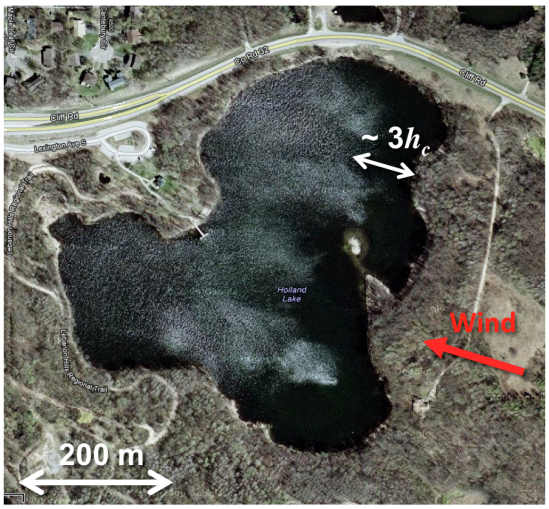

FIG. 8: Aerial photo of a small lake exhibiting light reflection off surface waves. A sheltered region with no wave field near shore (Source: USGS)

3.2 *Surface Shear Stress Recovery*

Figure 9 shows direct measurements in the wind tunnel of surface shear stress recovery downwind of the reattachment for the BFS and Canopy-BFS cases using the Preston tube method. The data shows a wide range of shear stress rates. The shear downwind of the BFS recovers much more quickly than downwind of the Canopy-BFS. Surface shear stress reaches 90% of τ_0 after about $30h_c$ downwind of the BFS, but requires about 70-80h_c downwind of the Canopy-BFS.

The shear stress recovery immediately downwind of reattachment can in first approximation be characterized by an exponential function of the form

$$\frac{\tau}{\tau_0} = 1 - \Delta\tau_c exp\left[(1-(x-x_r))/(x_r/\alpha)\right], \qquad (7)$$

where τ_0 is the shear stress after equilibrium, $\Delta\tau_c$ is the difference between the shear stress at the surface at equilibrium and within the canopy and α is a constant that depends on canopy height, density and boundary layer thickness.

4. Discussion and Conclusions

An empirically derived model for the parameterization of wind sheltering of a small lake in flat terrain and surrounded by a tree canopy has been developed to predict the correction for 1-D delivery of TKE by wind shear to a lake surface. The model has been shown to work reasonably well in many cases compared to wind sheltering coefficients determined by lake temperature model calibration.

Table 2: Separation and reattachment scales from experiments

Configuration	x_s/h_c	x_r/h_c
BFS	0	6.2
Canopy-BFS	0.5	2.6
Canopy-Patch	1	8.2
Solid Block	0	4.6

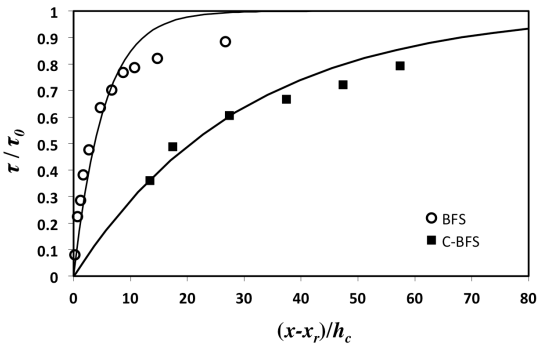

FIG. 9: Plot of surface shear stress recovery downwind of reattachement

For small lakes, where the specific structure of the canopy and other wind sheltering elements becomes important, we have shown through controlled wind tunnel experiments that not only canopy height, but also canopy length and canopy density affect the separation and reattachment of the ABL. The reattachment length for a solid BFS is about $6h_c$ and for a Canopy-BFS, with a canopy density of $a = 10$ m^{-1}, about $x_r = 2.6h_c$. In other experiments the reattachment was delayed by the limited length of the canopy patch. The longest distances for reattachment were obtained for canopy patches about 2 times the canopy height. Thermal stability for the canopy patch extended the point of reattachment up to $x_r = 11h_c$. This large range of reattachment scales has an impact on the shear stress recovery.

After the flow reattaches, a new boundary layer develops over the lake surface. The canopy density affects surface shear stress recovery in the developing equilibrium layer over the water surface. Shear stress recovers faster for the solid BFS than for the Canopy-BFS case.

Future work to analyze data collected for different canopy lengths as well as thermal stability effects on the ABL transition will help elucidate the range of reattachment scales which can be expected. Scalar transport in the reattachment and downwind developing region will also be studied both in controlled experiments as well as over a small lake in the field. Wind and flux measurements at a sheltered Trout Lake in Northern Minnesota will be used to characterize wind field variability and fluxes.

Acknowledgements

This research was supported by the Swiss National Foundation (grant 200021-132122), the National Science Foundation (grant ATM-0854766), and NASA (grant NNG06GE256). C.M. would like to acknowledge funding from NSF IGERT (Grant DGE-0504195) and NASA Earth and Space Science Fellowship (Grant NNX10AN52H). E.R. was partially supported by the USGS (Grant GC11NQ00DRD0000 - 8607DRD - MN 258). Thanks also go to the research engineer Jim Tucker for his efforts in preparation of the experimental facility and instruments. Computing resources were provided by the Minnesota Super-

computing Institute (MSI) and by a grant from the Swiss National Supercomputing Center (CSCS) under project ID s306.

References

Belcher, S.E., N. Jerram, and J.C.R. Hunt (2003) Adjustment of a turbulent boundary layer to a canopy of roughness elements, *J Fluid Mech* **488**, 369–398.

Belcher, S.E., I.N. Harman, and J.J. Finnigan (2012) The Wind in the Willows: Flows in Forest Canopies in Complex Terrain, *Ann Rev Fluid Mech* **44**, 479–504.

Detto, M., G.G. Katul, M.B. Siqueira, J.-Y. Juang, and P. Stoy (2008) The structure of turbulence near a tall forest edge: The backward-facing step flow analogy revisited, *Ecol. Appl.*, **18**(6), 14201435, doi:10.1890/ 06-0920.1.

Downing, J. A., et al. (2006) The global abundance and size distribution of lakes, ponds, and impoundments, *Limnol. Oceanogr.*, **51**(5), 23882397.

Driver, D.M. and Seegmiller, H.L. (1985) Features of a Reattaching Turbulent Shear Layer in Divergent Channel Flow, *AIAA Journal*, **23**(2), 163-171.

Dupont, S. and Y. Brunet (2009) Coherent structures in canopy edge flow: a large-eddy simulation study, *J Fluid Mech*, **630**, 93–128.

Garratt, J.R. (1994) *The atmospheric boundary layer*, Cambridge University Press.

Fang, X., S.R. Alam, P. Jacobson, D. Preira and H.G. Stefan (2010) Simulations of water quality in Cisco lakes in Minnesota, St. Anthony Falls Laboratory *Rep.* **544**. University of Minnesota.

Finnigan, J.J. (2000) Turbulence in plant canopies, *Annu Rev Fluid Mech* **32**, 519–571.

Ghisalberti, M. (2009) Obstructed shear flows: similarities across systems and scales, *J Fluid Mech* **641**, 51–61.

Jiang, L.P., X. Fang, H.G. Stefan, P.C. Jacobson and D.L. Pereira (2012) Oxythermal habitat parameters and identifying cisco refuge lakes in Minnesota under future climate scenarios using variable benchmark periods, *Ecological Modeling* **232**, 14–27.

Markfort, C.D., A.L.S. Perez, J.W. Thill, D.A. Jaster, F. Porte-Agel, and H.G. Stefan (2010) Wind sheltering of a lake by a tree canopy or bluff topography, *Water Resour. Res.*, **46**, W03530, doi:10.1029/2009WR007759.

Stefan, H.G. and D.E. Ford (1975) Temperature Dynamics of Dimictic Lakes, *Journal Hydraulic Div.*, ASCE, **101**(HY1), 97–114.